Inorganic Chemistry

Article

pubs.acs.org/IC

Structural Diversity and Photoluminescent Properties of Zinc Benzotriazole-5-carboxylate Coordination Polymers

Juan Liu,[†,§] Hua-Bin Zhang,[†] Yan-Xi Tan,[†] Fei Wang,[†] Yao Kang,[†] and Jian Zhang*[,†,‡]

[†]State Key Laboratory of Structural Chemistry, Fujian Institute of Research on the Structure of Matter, Chinese Academy of Science, 350002 Fuzhou, P. R. China

[‡]College of Materials & Chemical Engineering, China Three Gorges University, Yichang 443002, P. R. China

[§]University of Chinese Academy of Science, 100049 Beijing, P. R. China

Supporting Information

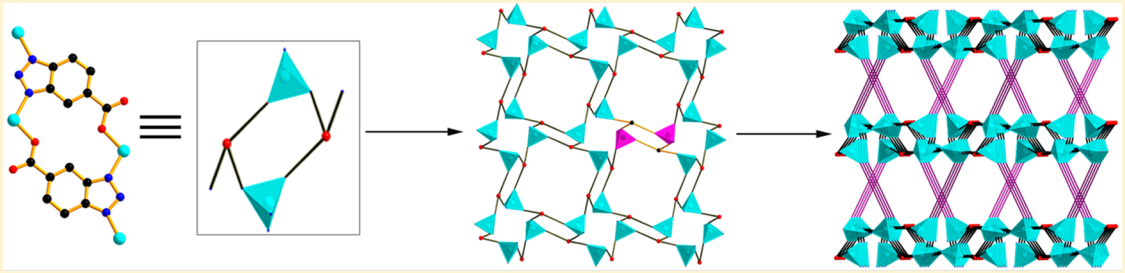

ABSTRACT: A series of zinc(II) compounds, $[Zn_2(btca)_2(im)_2]\cdot(DMA)$ (**1**; H_2btca = benzotriazole-5-carboxylate acid, im = imidazole, and DMA = *N*,*N*-dimethylacetamide), $[Zn(btca)(im)]\cdot(DMF)$ (**2**; DMF = *N*,*N*-dimethylformamide), $[Zn_2(btca)_2(tmdpy)]\cdot 2(DMF)\cdot 5(H_2O)$ [**3**; tmdpy = 1,3-di(4-pyridyl)propane], and $[H_2N(CH_3)_2]_2[Zn_3(btca)_4]\cdot(DMF)$ (**4**), have been successfully synthesized via rational control of experimental conditions. Single-crystal X-ray diffraction analyses indicate that compounds **1** and **2** are isomers, and both of them exhibit two-dimensional structures with the same uninodal 3-connected **fes** topology. Additionally, the three-dimensional (3D) structure of **3** was obtained by using tmdpy instead of an im ligand under synthesis conditions similar to those of compound **2**. Interestingly, compound **3** presents a pillared-layer structure with a (3,4)-connected $(4.8^2.10^3)(4.8^2)$ topology. When 4,4′-bipyridine was used to replace tmdpy, the assembly between Zn^{2+} ions and H_2btca ligands produced a chiral 3D framework of **4**. Furthermore, compound **4** showed a new (3,4)-connected topology with a vertex symbol of $(4.6.8^4)_2(4.6.8)(4.8^2)(6.8^2)_2(6.8^5)$. A comparison of all compounds suggested that the structural diversity of the compounds could be tuned by altering the auxiliary ligand. In addition, the photoluminescent properties of compounds **1**−**4** were measured.

1. INTRODUCTION

Metal−organic frameworks (MOFs) have attracted tremendous attention because of their intriguing structural diversity and potential applications in molecular recognition, ion exchange, adsorption, fluorescence, and catalysis.[1] Although many MOFs with various structures and properties have been synthesized in various ways and strategies over the past two decades,[2] obtaining a desirable MOF with unique structure and function is still a challenge because many factors such as the reaction temperature, solvents, templates, pH, metal ions, and organic ligands may affect the self-assembly of MOFs.[3] Therefore, understanding the assembly process between metal centers and organic ligands is crucial for obtaining a target MOF.

Currently, multidentate N-donor or O-donor ligands have been widely used for the construction of MOFs with various structures.[4−6] Herein, the benzotriazole-5-carboxylate (btca) ligand, which has been less explored in the development of novel coordination networks,[7] is chosen as an organic linker to synthesize new functional MOFs. The btca ligand with a 1,2,3-triazole ring and carboxyl group may lead to the formation of MOFs with special secondary building units (SBUs). Moreover, the relatively large π-conjugated system in the benzotriazole ring not only might contribute much to the desirable luminescent property but also might strengthen the stability of the structures.[8]

In this work, four interesting Zn−btca compounds, $[Zn_2(btca)_2(im)_2]\cdot(DMA)$ (**1**; im = imidazole, DMA = *N*,*N*-dimethylacetamide), $[Zn(btca)(im)]\cdot(DMF)$ (**2**; DMF = *N*,*N*-dimethylformamide), $[Zn_2(btca)_2(tmdpy)]\cdot 2(DMF)\cdot 5(H_2O)$ [**3**; tmdpy = 1,3-di(4-pyridyl)propane], and $[H_2N(CH_3)_2]_2[Zn_3(btca)_4]\cdot(DMF)$ (**4**), were successfully synthesized. All compounds contain a SBU of $[Zn_2(btca)_2]$, and the SBUs further link each other into diverse 3-connected layers through different assembling modes. Compounds **1** and **2** have similar two-dimensional (2D) networks with a 3-connected **fes** topology; the structure of **2** contains one-dimensional (1D) channels along the *c*-axis, and compound **1** is a dense structure.

Received: September 30, 2013
Published: January 10, 2014

   dx.doi.org/10.1021/ic402467g | *Inorg. Chem.* 2014, 53, 1500−1506

Table 1. Crystal Data and Structure Refinement for 1−4

	1	2	3	4
formula	$C_{24}H_{23}N_{11}O_5Zn_2$	$C_{13}H_{14}N_6O_3Zn$	$C_{27}H_{20}N_8O_4Zn_2$	$C_{28}H_{12}N_{12}O_8Zn_3$
fw	676.27	367.69	651.25	840.61
crystal system	orthorhombic	orthorhombic	tetragonal	monoclinic
space group	$Pna2_1$	$Pccn$	$P4/ncc$	$P2_1$
a (Å)	16.6901(11)	14.531(2)	18.1524(7)	10.1264(10)
b (Å)	8.1097(13)	21.960(2)	18.1524(7)	15.0101(8)
c (Å)	20.2890(12)	9.8361(14)	27.5897(16)	17.4862(18)
β (deg)	90	90	90	106.36(6)
V (Å^3)	2746.2(5)	3138.7(7)	9091.1(9)	2550.3(4)
Z	4	8	8	2
D_c (g/m^3)	1.636	1.556	0.952	1.095
μ (mm^{-1})	1.804	1.589	1.085	1.443
R_{int}	0.0869	0.0470	0.1181	0.0730
GOF	0.954	1.008	0.946	0.970
R_1, wR_2 [$I > 2\sigma(I)$]	0.0741, 0.0987	0.0546, 0.1346	0.0883, 0.2108	0.0597, 0.1633
R_1, wR_2 (all data)	0.1486, 0.1185	0.0900, 0.1533	0.1833, 0.2380	0.0744, 0.1794

Compound **3** presents a three-dimensional (3D) pillared-layer framework with a new (3,4)-connected topology. Interestingly, compound **4** is a 3D chiral porous framework constructed from rigid achiral ligands. The topology of **4** is also a new (3,4)-connected net. The luminescence properties of compounds **1**−**4** have been characterized. The porosity of compounds **2** and **3** was confirmed by gas adsorption experiments.

2. EXPERIMENTAL METHODS

Materials and Methods. Powder X-ray diffraction (PXRD) analyses were conducted with a MiniFlex II diffractometer with Cu Kα radiation (λ = 1.54056 Å), with a step size of 0.05°. Elemental analyses of C, H, and N were measured on a Vario MICRO E III elemental analyzer. The IR spectra (KBr pellets) were recorded on a Magna 750 FTIR spectrophotometer. Thermogravimetric analyses (TGAs) were conducted on a NETSCHZ STA-449C thermoanalyzer at a heating rate of 10 °C/min under a N_2 atmosphere. Solid fluorescence properties were measured at room temperature with a HORIBA Jobin-Yvon FluoroMax-4 spectrometer. The topologies of all compounds were analyzed with TOPOS version 4.0.[9]

Synthesis of $[Zn_2(btca)_2(im)_2]\cdot$(DMA) (1). A mixture of $ZnCl_2$ (0.5 mmol, 71.3 mg), H_2btca (0.5 mmol, 82.5 mg), imidazole (0.5 mmol, 34.4 mg), DMA (4.0 mL), and H_2O (2.0 mL) was added to a 25 mL vial. The vial was sealed, held at 120 °C for 3 days, and then cooled to room temperature. Colorless crystals of **1** were obtained in 82% yield based on H_2btca. Anal. Calcd for **1**: C, 42.62; H, 3.43; N, 22.78. Found: C, 42.58; H, 3.71; N, 23.26. IR (KBr pellet): 3268(w), 3144(w), 2941(w), 2854(w), 1621(s), 1650(m) 1371(w), 1273(m), 1254(m), 1178(m) 1150(s), 1071(s), 1005(m), 956(m), 909(m), 840(m), 792(s), 755(s), 706(m), 658(m), 601(m) cm^{-1}.

Synthesis of [Zn(btca)(im)]·(DMF) (2). Colorless crystals of **2** were obtained in 75% yield based on H_2btca by a procedure similar to that used for **1** except that DMA was replaced by DMF. Anal. Calcd for **2**: C, 42.46; H, 3.84; N, 22.86. Found: C, 41.25; H, 3.77; N, 23.12. IR (KBr pellet): 3124(w), 3076(w), 2961(w), 2874(w), 1612(w), 1573(w), 1516(s), 1477(m) 1400(w), 1323(s), 1275(s), 1159(s), 1101(s), 1072(s), 957(s), 909(m), 832(m), 784(s), 755(s), 706(s) 658(s), 600(s), 571(m) cm^{-1}.

Synthesis of $[Zn_2(btca)_2(tmdpy)]\cdot 2(DMF)\cdot 5(H_2O)$ (3). A mixture of $ZnCl_2$ (0.5 mmol, 72.5 mg), H_2btca (0.5 mmol, 7.90 mg), tmdpy (0.5 mmol, 10.34 mg), DMF (4.0 mL), and H_2O (2.0 mL) was added to a 25 mL vial. The vial was sealed, held at 120 °C for 3 days, and then cooled to room temperature. Colorless crystals of **3** were obtained in 88% yield based on H_2btca. Anal. Calcd for **3**: C, 44.66; H, 5.00; N, 15.78. Found: C, 44.51; H, 4.77; N, 15.68. IR (KBr pellet): 3442(w), 3047(w), 2941(w), 2854(w), 1612(s), 1554(m), 1506(m), 1438(s), 1361(m), 1275(m), 1217(m), 1150(m), 1072(s), 1034(s), 861(m), 822(s), 784(s), 706(m), 620(m), 514(m) cm^{-1}.

Synthesis of $[H_2N(CH_3)_2]_2[Zn_3(btca)_4]\cdot$(DMF) (4). A mixture of $ZnCl_2$ (0.25 mmol, 48.2 mg), H_2btca (0.25 mmol, 43.8 mg), 4,4-bipy (0.25 mmol, 40.5 mg), DMF (3.0 mL), and H_2O (3.0 mL) was added to a 25 mL vial. The vial was sealed, held at 120 °C for 3 days, and then cooled to room temperature. Colorless crystals of **4** were obtained in 40% yield based on H_2btca. Anal. Calcd for **4**: C, 41.96; H, 3.12; N, 20.97. Found: C, 41.91; H, 3.27; N, 20.93. IR (KBr pellet): 3403(w), 3095(w), 2922(w), 2363(w), 1660(s), 1621(m), 1593(s), 1564(s), 1487(m), 1400(s), 1275(m), 1188(m), 1092(m), 1034(m), 957(m), 899(m), 793(s), 755(s), 706(s), 658(m), 601(m), 552(m) cm^{-1}.

X-ray Crystallographic Analysis. The diffraction data for **1**−**4** were collected on an Oxford Xcalibur diffractometer equipped with graphite-monochromatized Mo Kα radiation (λ = 0.71073 Å) at 293(2) K. The structures were determined by direct methods and refined on F^2 full-matrix least-squares using the SHELXTL-97 program package.[10] All non-hydrogen atoms were refined anisotropically except N6, C60−C62, and O3 in **2** and C8−C11 and C14 in **3**, which were refined isotropically. The restraints (SIMU, DFIX, DANG, and FLAT) were applied in **3**. PLATON was used for the calculation of guest available volumes, and the squeeze option was used for disordered and unlocated anions and guest molecules.[11] In **3**, solvent molecules could not be located; thus, the squeeze option was used in the final refinement. In **4**, the $H_2N(CH_3)_2^+$ ions and solvent molecules were disordered and refined using the squeeze option in the final refinement. According to TGA and element analysis, two DMF molecules and five water molecules per formula can be confirmed in **3**, and the number of solvent molecules of compound **4** was proposed to be approximately one DMF per formula. Crystal data for the compounds are summarized in Table 1.

3. RESULTS AND DISCUSSION

Structure Description. *$[Zn_2(btca)_2(im)_2]\cdot$(DMA) (1).* Single-crystal X-ray diffraction analysis showed that compound **1** crystallized with orthorhombic symmetry in noncentrosymmetric space group $Pna2_1$. In the structure of **1**, each asymmetric unit contains two crystallographically independent Zn(II) centers, two btca ligands, two im ligands, and a DMA molecule. Both Zn(II) centers show similar tetrahedral coordination geometry (Figure 1a), and each Zn(II) center is coordinated by a carboxylate oxygen atom from a btca ligand and three nitrogen atoms from two distinct btca ligands and an im ligand. The btca ligand acts as a μ_3-bridging ligand and links three Zn(II) ions. Two btca ligands and two Zn(II) ions form a

dx.doi.org/10.1021/ic402467g | Inorg. Chem. 2014, 53, 1500−1506

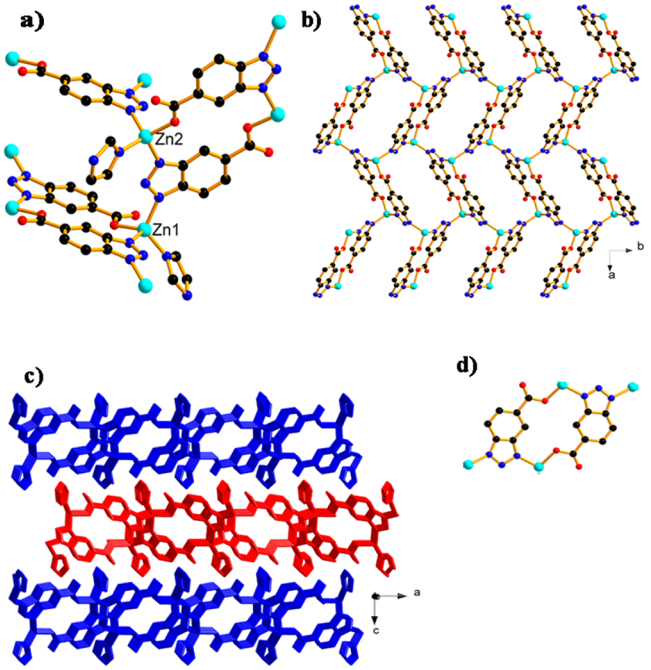

Figure 1. (a) Coordination environment around the Zn atoms in **1**. (b) The 3-connected layer in **1** viewed from the *c*-axis. (c) A−B−A stacking mode of the layers in **1**. (d) $Zn_2(btca)_2$ building unit.

$Zn_2(btca)_2$ building unit (Figure 1d). The $Zn_2(btca)_2$ building units further link each other into a 3-connected layer (Figure 1b). The 3-connected layer is prevented from forming a higher-order dimensional network by the terminal im ligands that hang beside the two sides of the layer (Figure 1c). The resulting layers are parallel to each other and stack into a 3D dense framework with an A−B−A mode (Figure 1c). No obvious interactions are observed between the layers. In **1**, the btca ligands and Zn ions are both 3-connected nodes. The whole framework can be topologically represented as a uninodal 3-connected **fes** net with a Schläfli symbol of $(4, 8^2)$ (Figure S2a of the Supporting Information).

*[Zn(btca)(im)]·(DMF) (**2**).* Compound **2** crystallized in orthorhombic space group *Pccn*. Different from the case for **1**, there is only one crystallographically independent Zn(II) center in the asymmetric unit in **2**. As shown in Figure 2a, the Zn(II) center presents a tetrahedral coordination geometry, which is coordinated by a carboxylate oxygen atom from a btca ligand and three nitrogen atoms from two distinct btca ligands and an im ligand. The $Zn_2(btca)_2$ SBUs link each other into a 3-connected wavelike layer (Figure 2b). The wavelike layer is prevented from being a 3D framework by terminal im ligands that hand along the two sides of the layer (Figure 2c). The resulting layers are parallel to each other and packed into a 3D pillared-layer structure with 1D channels along the *c*-axis. There are rich N−H···O hydrogen bonds between adjacent layers [$d_{N\cdots O}$ = 2.698(10) Å] (Figure 2d). The packing mode of wavelike layers is also an A−B−A mode (Figure 2c). The 1D channels are filled with DMF molecules (Figure S1 of the Supporting Information). The structure of **2** has 37.9% solvent-accessible volume as identified by PLATON. The topology of **2** is the same as that of **1**, which is also a 3-connected **fes** net (Figure S2b of the Supporting Information). When considering the hydrogen bonds in **2**, the btca ligands and Zn(II) ions both become 4-connected nodes, so the topology becomes a 4-

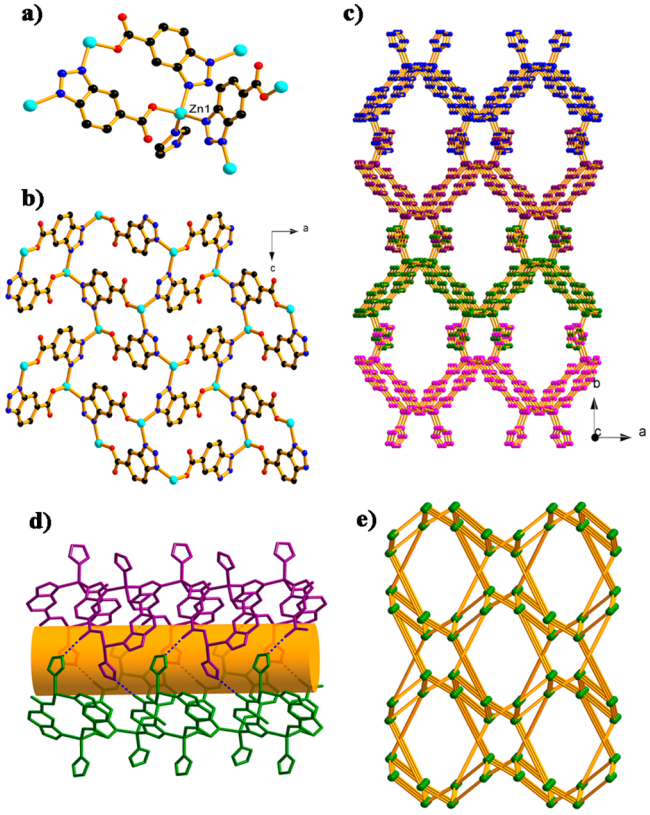

Figure 2. (a) Coordination environment around the Zn atom in **2**. (b) The 3-connected wavelike layer in **2** viewed from the *b*-axis. (c) The layers stack into a 3D pillared-layer framework via hydrogen bonding interactions. (d) N−H···O hydrogen bonding interactions in **2**. (e) The 4-connected topology of **2**.

connected one. The Schläfli symbol of this new topological net is 4.8^5.

Although **2** possesses the same ligands as **1** and a coordination mode similar to that of **1**, the structure of **2** is different from that of **1** because the angles between $Zn_2(btca)_2$ building units in **2** are different from those in **1**. The angles between $Zn_2(btca)_2$ units in **1** make the layer of **1** a flat one, but the angles between $Zn_2(btca)_2$ units in **2** make the layer of **2** a wavelike one.

*[$Zn_2(btca)_2(tmdpy)$]·2(DMF)·5(H_2O) (**3**).* Compound **3** crystallized in the tetragonal system in space group *P*4/*ncc*. Its asymmetric unit contains only one crystallographically independent Zn(II) center. As shown in Figure 3a, Zn1 exhibits a tetrahedral geometry and is coordinated by a carboxylate oxygen atom from a btca ligand and three nitrogen atoms from two distinct btca ligands and a tmdpy ligand. In **3**, the $Zn_2(btca)_2$ building unit is constructed and a **fes**-type layer is produced, as well (Figure 3b). Then the μ_2-tmdpy ligands link the layers into a pillared-layer framework (Figure 3c), which exist as 1D tubular channels with a window size of 8.831 Å × 8.831 Å along the *c*-axis (Figure 3d). An approximately 46.2% solvent-accessible volume was calculated by PLATON. Because each btca ligand acts as a 3-connected node and each Zn(II) ion is a 4-connected node, the framework of **3** presents a (3,4)-connected net (Figure 3e). The vertex symbol of this new net is $(4.8^2.10^3)(4.8^2)$, which is analyzed by TOPOS version 4.0.

*[$H_2N(CH_3)_2]_2[Zn_3(btca)_4]$·(DMF) (**4**).* Compound **4** crystallized in the chiral $P2_1$ space group. In the asymmetric unit of **4**, there are three independent Zn(II) ions, all of which are four-

dx.doi.org/10.1021/ic402467g | *Inorg. Chem.* 2014, 53, 1500−1506

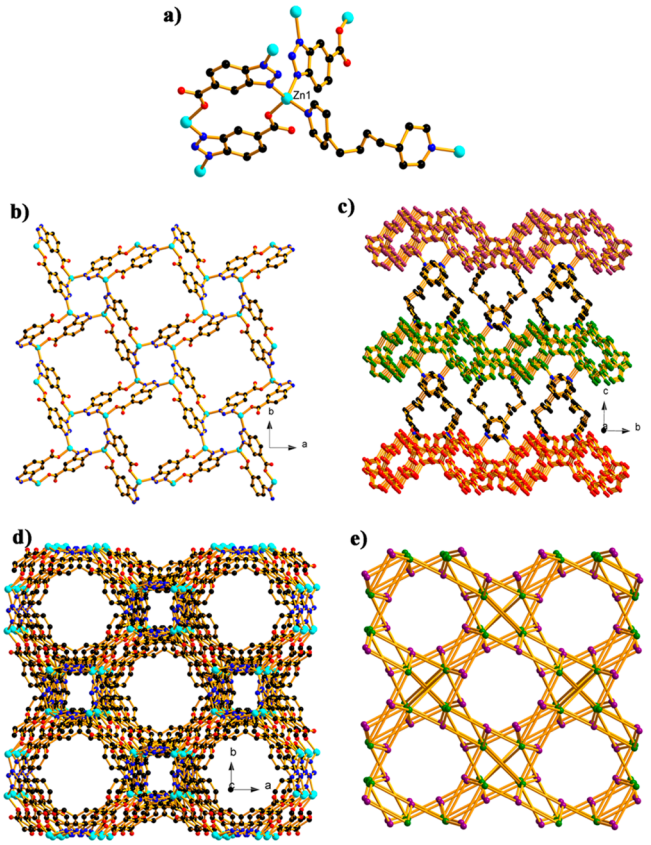

Figure 3. (a) Coordination environment around the Zn atoms in **3**. (b) Layer in **3**. (c) Layers linked into a pillared-layer structure by tmdpy. (d) 1D channel in **3** along the *c*-axis. (e) The (3,4)-connected topology of **3**. The purple nodes represent the 3-connected btca ligands and the green nodes the 4-connected Zn(II) ions.

coordinate. As shown in Figure 4a, Zn1 and Zn2 are in similar coordination environments. Each of them is coordinated by a carboxylate oxygen atom from a btca ligand and three nitrogen atoms from two distinct btca ligands. Zn3 is coordinated by two carboxylate oxygen atoms from two different btca ligands and two nitrogen atoms from two distinct btca ligands. Zn1 and Zn2 are linked by the μ_3-bridging btca ligands into a **fes**-type wavelike layer, and the Zn3 ions are linked by the btca ligands into a 4-connected chiral layer (Figure 4b,c). The 4-connected layers link **fes**-type layers into a final 3D pillared-layer structural framework (Figure 4e). In **4**, the btca ligands are 3-connected nodes and the Zn ions are 4-connected nodes, so the whole framework can be topologically represented as a (3,4)-connected net (Figure 4f). Notably, this topology with a vertex symbol of $(4.6.8^4)_2(4.6.8)(4.8^2)(6.8^2)_2(6.8^5)$ is a new one. The solvent-accessible volume of **4** is estimated by PLATON to be ~30.8% of the total crystal volume.

The chirality in the structure of **4** is worth noting. The chirality of **4** may be generated from the 4-connected layers constructed from Zn3 and btca ligands (Figure 4b,c). Although the btca ligand is achiral, the 4-connected layer is a chiral layer built from helix Zn−btca chains (Figure 4d). Solid-state circular dichroism (CD) measurements were performed on solid material in KBr plates to illustrate the chiral nature of **4**, and groups of randomly selected single crystals of **4** were used for the CD spectrum. As shown in Figure 5, it displays opposite Cotton effects,[12] which reveals that single crystal of **4** is homochiral but the bulk sample may be racemic.

Structural Diversity of the Four Compounds. By tuning the synthesis conditions and auxiliary ligands, we obtained four new Zn−btca compounds with 2D and 3D structures. Compounds **1** and **2** with similar 2D structures were synthesized by the same agents but in different solvents. Moreover, different auxiliary ligands that were used for the synthesis resulted in the formation of different structures. To explain the effects of auxiliary ligands on the diversity of these compounds, the charge balance of the four compounds is considered. These four compounds all possess a neutral layer structure composed of the same building block $Zn_2(btca)_2$, and the layers are isomers. The coordination modes of the metal centers and the ligands in four compounds of the layers are almost the same. To further link these layers into neutral frameworks, the coligand should be neutral. In **1** and **2**, im acts as a terminal neutral ligand to prevent the layer from forming a 3D framework. In **3**, tmdpy is a neutral bridging ligand and links the adjacent neutral layers into a 3D framework (Figure 3c). In compound **4**, although the achiral neutral **fes**-type layers are linked by anionic chiral layers into a 3D framework, the $[H_2N(CH_3)_2]^+$ ions balance the negative charge of the framework.

Thermal Stability. TGA of compounds **1**−**4** was performed to investigate their thermal behavior in a N_2 atmosphere from 28 to 600 °C at a heating rate of 10 °C/min (Figure S7 of the Supporting Information). Before the TGA test, the phase purity of all compounds was characterized by powder X-ray diffraction (Figures S3−S6 of the Supporting Information). The TGA curve demonstrated that compound **1** was stable up to 300 °C and then decomposed upon being heated further (Figure S7 of the Supporting Information). TGA of compound **2** showed a weight loss of 19.8% in the range of 30−245 °C, implying the removal of a free DMF molecule (calcd, 19.9%) per formula unit. For **3**, the first weight loss of 10.6% in the range of 25−116 °C indicated the exclusion of free water molecules and the second weight loss of 15.2% between 116 and 240 °C could be attributed to the loss of DMF molecules. For **4**, the first weight loss of 4.5% in the temperature range of 28−67 °C indicated the surface absorption of moisture and the second weight loss of 16.8% between 113 and 300 °C was attributed to the loss of a free DMF molecule and a $H_2N(CH_3)_2^+$ ion per formula unit (calcd, 16.1%).

It is worth noting that compound **2** has excellent thermal stability. As shown in Figure S5 of the Supporting Information, no weight loss can be observed between 245 and 390 °C. When compound **2** was treated at 200 or 300 °C, the PXRD patterns of the treated samples were very much in agreement with the simulated pattern of **2** (Figure 6). The result suggested that the desolvated framework can keep its crystalline state even at high temperatures.

Gas Adsorption. To evaluate the porosity of **2** and **3**, gas adsorption isotherms were measured with N_2. Both of the samples were activated in methanol for 3 days and then evacuated under high dynamic vacuum at room temperature for 24 h. Compound **2** exhibits a type I isotherm of N_2 sorption at 77 K and 1 bar (Figure 7a). The Langmuir surface area, BET surface area, and pore volume of **2** are 473 m^2/g, 340 m^2/g, and 0.17 cm^3/g, respectively. Compound **3** also exhibits a type I isotherm of N_2 sorption at 77 K and 1 bar (Figure 7b). The Langmuir surface area, BET surface area, and pore volume of **3** are 529 m^2/g, 378 m^2/g, and 0.21 cm^3/g, respectively.

dx.doi.org/10.1021/ic402467g | Inorg. Chem. 2014, 53, 1500−1506

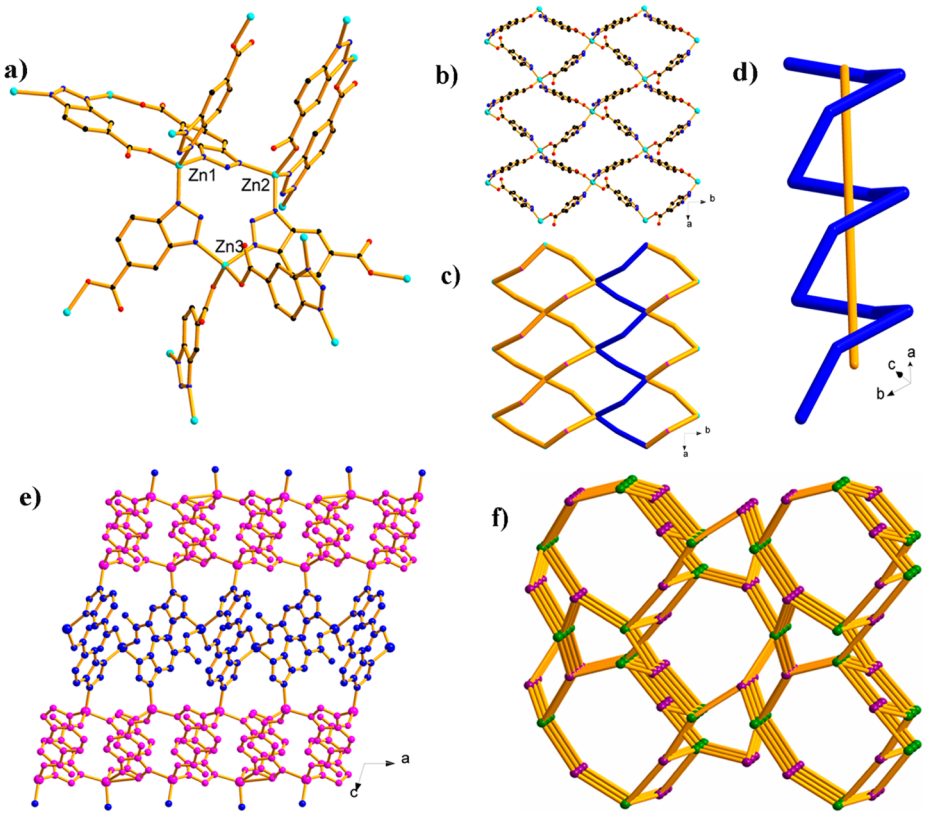

Figure 4. (a) Coordinated environment of Zn(II) in **4**. (b and c) The 4-connected chiral layer of $(Zn-btca)_n$ in **4**. (d) Helix chain of the chiral layer. (e) The 4-connected layers link 3-connected layers into a 3D pillared-layer structure of **4**. (f) The (3,4)-connected topology of **4**. The purple nodes represent the 3-connected btca ligand and the green nodes the 4-connected Zn(II) ions.

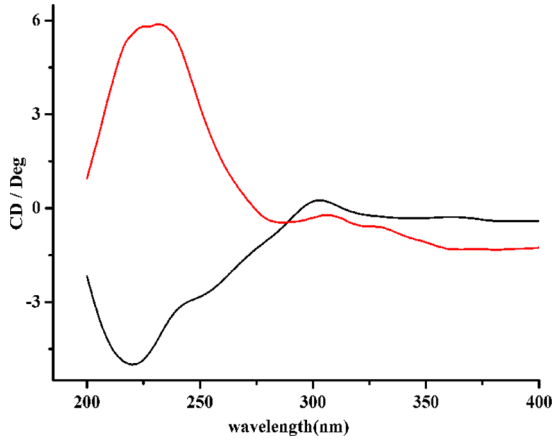

Figure 5. Solid-state CD spectra of compound **4**.

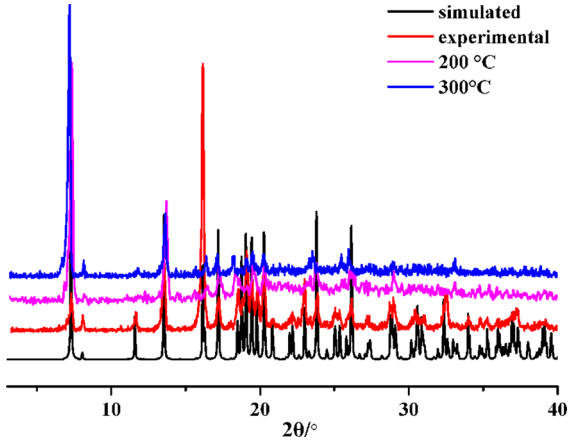

Figure 6. PXRD patterns of **2**: simulated (black), measured (red), and desolvated by heating at 200 °C (pink) and 300 °C (blue).

Photoluminescent Properties. As a series of d^{10} metal–organic hybrid coordination polymers, **1**–**4** via their solid-state emission spectra together with the ligand H_2btca and the N-donor auxiliary ligands used in this work have been investigated at room temperature. As shown in Figure 8, the emission spectra of **1** display two peaks at 395 and 410 nm under 362 nm excitation (Figure S8 of the Supporting Information), and the emission spectra of **3** contain two peaks at 418 and 500 nm; these bands of **1** and **3** are consistent with the emission wavelength of the ligand H_2btca and auxiliary ligands (im for **1** and tmdpy for **3**). Therefore, the photoluminescent emission of **1** and **3** may be assigned to ligand–ligand charge transfer (LLCT).[8,13] Excitation at 345 nm leads to an intense blue fluorescent emission band at 382 nm for **2**, which can be assigned to intraligand ($\pi-\pi^*$) fluorescent emission of the ligand H_2btca. Similar to compounds **1** and **3**, compound **4** also displays two emission bands at 416 and 485 nm under 340 nm excitation, as its structure contains only one ligand, its emission behavior can be tentatively assigned to the coexistence of intraligand fluorescent emissions and LMCT.[8,14]

4. CONCLUSIONS

In summary, four new Zn(II) coordination polymers based on the btca ligands were synthesized and structurally characterized. Interestingly, compound **4** presented a chiral framework with

dx.doi.org/10.1021/ic402467g | Inorg. Chem. 2014, 53, 1500–1506

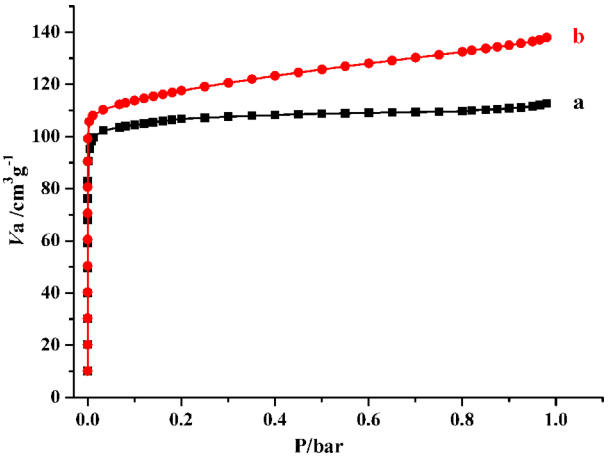

Figure 7. N_2 sorption isotherms at 77 K for compounds **2** (a) and **3** (b).

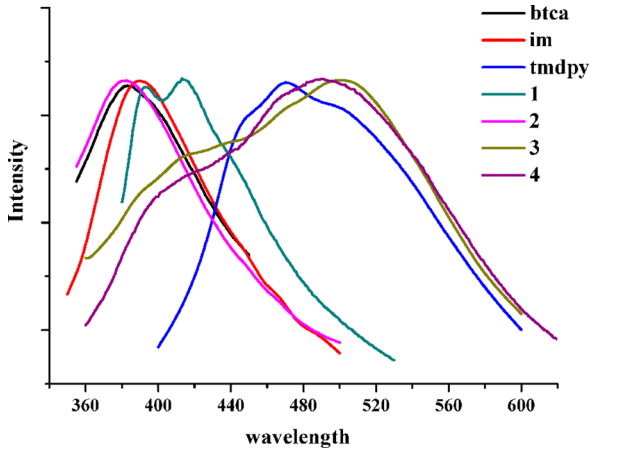

Figure 8. Emission spectra of compounds **1**–**4** and the organic ligands at room temperature.

only an achiral ligand. Structural comparisons of these four compounds demonstrated that the structural diversity of MOFs can be controlled by reasonable selection of auxiliary ligands. In addition, such compounds display modest thermal stability and solid-state luminescent emission.

■ ASSOCIATED CONTENT

Ⓢ Supporting Information

Additional figures, TGA, powder X-ray diffraction patterns, and a CIF file. This material is available free of charge via the Internet at http://pubs.acs.org.

■ AUTHOR INFORMATION

Corresponding Author

*E-mail: zhj@fjirsm.ac.cn.

Notes

The authors declare no competing financial interest.

■ ACKNOWLEDGMENTS

We are grateful for the support of this work by the 973 program (2012CB821705 and 2011CB932504), NSFC (91222105 and 21221001), and CAS (XDA07070200).

■ REFERENCES

(1) (a) Pramanik, S.; Zheng, C.; Emge, T. J.; Li, J. *J. Am. Chem. Soc.* **2011**, *133*, 4153–4155. (b) Jiang, H.-L.; Xu, Q. *Chem. Commun.* **2011**, *47*, 3351–3370. (c) Zhao, D.; Timmons, D. J.; Yuan, D.-Q.; Zhou, H.-C. *Acc. Chem. Res.* **2011**, *44*, 123–133. (d) Zhang, H.-X.; Wang, F.; Yang, H.; Tan, Y.-X.; Zhang, J.; Bu, X.-H. *J. Am. Chem. Soc.* **2011**, *133*, 11884–11887. (e) Wang, F.; Liu, Z.-S.; Yang, H.; Tan, Y.-X.; Zhang, J. *Angew. Chem., Int. Ed.* **2011**, *50*, 450–453. (f) Song, F.-J.; Wang, C.; Falkowski, J. M.; Ma, L.-Q.; Lin, W.-B. *J. Am. Chem. Soc.* **2010**, *132*, 15390–15398.

(2) (a) Férey, G. *Chem. Soc. Rev.* **2008**, *37*, 191–214. (b) Long, J. R.; Yaghi, O. M. *Chem. Soc. Rev.* **2009**, *38*, 1213–1214. (c) Stock, N.; Biswas, S. *Chem. Rev.* **2012**, *112*, 933–969. (d) Perry, J. J., IV; Perman, J. A.; Zaworotko, M. J. *Chem. Soc. Rev.* **2009**, *38*, 1400–1417.

(3) (a) Kanoo, P.; Gurunatha, K. L.; Maji, T. K. *Cryst. Growth Des.* **2009**, *9*, 4147–4156. (b) Sun, D.; Liu, F.-J.; Huang, R.-B.; Zheng, L.-S. *CrystEngComm* **2013**, *15*, 1185–1193. (c) Huang, X.-C.; Zhang, J.-P.; Chen, X.-M. *J. Am. Chem. Soc.* **2004**, *126*, 13218–13219. (d) Chen, M.; Chen, S.-S.; Okamura, T.; Su, Z.; Chen, M.-S.; Zhao, Y.; Sun, W.-Y.; Ueyama, N. *Cryst. Growth Des.* **2011**, *11*, 1901–1912. (e) Zhang, X.; Huang, Y.-Y.; Lin, Q.-P.; Zhang, J.; Yao, Y.-G. *Dalton Trans.* **2013**, *42*, 2294–2301. (f) Guo, F.; Wang, F.; Yang, H.; Zhang, X.; Zhang, J. *Inorg. Chem.* **2012**, *51*, 9677–9682.

(4) (a) Zhu, C.; Yuan, G.; Chen, X.; Yang, Z.; Cui, Y. *J. Am. Chem. Soc.* **2012**, *134*, 8058–8061. (b) Wu, T.; Zhang, J.; Zhou, C.; Wang, L.; Bu, X.; Feng, P.-Y. *J. Am. Chem. Soc.* **2009**, *131*, 6111–6113. (c) Lin, Q.; Wu, T.; Zheng, S.; Bu, X.; Feng, P. *Chem. Commun.* **2011**, *47*, 11852–11854. (d) Zeng, M.-H.; Wang, Q.-X.; Tan, Y.-X.; Hu, S.; Zhao, H.-X.; Long, L.-S. *J. Am. Chem. Soc.* **2010**, *132*, 2561–2563. (e) Guo, Z.; Wu, H.; Gadipelli, S.; Liao, T.; Zhou, Y.; Xiang, S.; Chen, Z.; Yang, Y.; Zhou, W.; O'Keeffe, M.; Chen, B. *Angew. Chem., Int. Ed.* **2011**, *50*, 3178–3181. (f) Liu, Y.; Boey, F.; Lao, L. L.; Zhang, H.; Liu, X.; Zhang, Q. *Chem.—Asian J.* **2011**, *6*, 1004–1006.

(5) (a) He, Y. P.; Tan, Y. X.; Wang, F.; Zhang, J. *Inorg. Chem.* **2012**, *51*, 1995–1997. (b) Li, J.-R.; Zhou, H.-C. *Nat. Chem.* **2010**, *2*, 893–898. (c) Yang, S.; Lin, X.; Blake, A. J.; Walker, G.; Hubberstey, P.; Champness, N. R.; Schröder, M. *Nat. Chem.* **2009**, *1*, 487–493. (d) He, Y.-P.; Tan, Y.-X.; Zhang, J. *Cryst. Growth Des.* **2013**, *13*, 6–9. (e) Ma, S.-Q.; Simmons, J. M.; Sun, D.-F.; Yuan, D.-Q.; Zhou, H.-C. *Inorg. Chem.* **2009**, *48*, 5263–5268. (f) Han, Y. F.; Li, X. Y.; Li, L. Q.; Ma, C. L.; Shen, Z.; Song, Y.; You, X. Z. *Inorg. Chem.* **2010**, *49*, 10781–10787. (g) Zhao, D.; Yuan, D.-Q.; Sun, D.-F.; Zhou, H.-C. *J. Am. Chem. Soc.* **2009**, *131*, 9186–9188. (h) Tan, Y. X.; He, Y. P.; Zhang, J. *Chem. Commun.* **2011**, *47*, 10647–10649.

(6) (a) Reinsch, H.; van der Veen, M. A.; Gil, B.; Marszalek, B.; Verbiest, T.; de Vos, D.; Stock, N. *Chem. Mater.* **2013**, *25*, 17–26. (b) Xiong, W.-W.; Athersh, E. U.; Ng, Y. T.; Ding, J.; Wu, T.; Zhang, Q. *J. Am. Chem. Soc.* **2013**, *135*, 1256–1259. (c) Zhuang, W.-J.; Ma, S.-Q.; Wang, X.-S.; Yuan, D.-Q.; Li, J.-R.; Zhao, D.; Zhou, H.-C. *Chem. Commun.* **2010**, *46*, 5223–5225. (d) Furukawa, H.; Ko, N.; Go, Y. B.; Aratani, N.; Choi, S. B.; Choi, E.; Yazaydin, A. Ö.; Snurr, R. Q.; O'Keeffe, M.; Kim, J.; Yaghi, O. M. *Science* **2010**, *239*, 424–428.

(7) (a) Zhang, X.-M.; Hao, Z.-M.; Zhang, W.-X.; Chen, X.-M. *Angew. Chem., Int. Ed.* **2007**, *46*, 3456–3459. (b) Uhl, W.; Vo, M.; Layh, M.; Rogel, F. *Dalton Trans.* **2010**, *39*, 3160–3162. (c) Lu, R.-Y.; Luan, G.-Y.; Han, Z.-B. *Acta Crystallogr.* **2010**, *C66*, m283–m284. (d) Xiao, J.; Liu, B.-Y.; Wei, G.; Huang, X.-C. *Inorg. Chem.* **2011**, *50*, 11032–11038.

(8) (a) Cui, Y.-J.; Yue, Y.-F.; Qian, G.-D.; Chen, B.-L. *Chem. Rev.* **2012**, *112*, 1126–1162. (b) Allendorf, M. D.; Bauer, C. A.; Bhakta, R. K.; Houk, R. J. T. *Chem. Soc. Rev.* **2009**, *38*, 1330–1352.

(9) Blatov, V. A. *IUCr CompComm Newsletter* **2006**, *7*, 4 (see also http://www.topos.ssu.samara.ru).

(10) Sheldrick, G. M. *Acta Crystallogr.* **2008**, *A64*, 112–122.

(11) Spek, A. L. *PLATON, A Multipurpose Crystallographic Tool*; Utrecht University: Utrecht, The Netherlands, 2005.

(12) Eliel, E. L.; Wilen, S. H. *Stereochemistry of Organic Compounds*; Wiley: New York, 1994; Chapter 13.

(13) (a) Chang, Z.; Zhang, A.-S.; Hu, T.-L.; Bu, X.-H. *Cryst. Growth Des.* **2009**, *9*, 4840−4846. (b) Wang, J.-J.; Hu, T.-L.; Bu, X.-H. *CrystEngComm* **2011**, *13*, 5152−5161.
(14) (a) Jiang, H.-L.; Liu, B.; Xu, Q. *Cryst. Growth Des.* **2010**, *10*, 806−811. (b) Qiu, Y.-C.; Li, Y.; Peng, G.; Cai, J.; Jin, L.; Ma, L.; Deng, H.; Zeller, M.; Batten, S. R. *Cryst. Growth Des.* **2010**, *10*, 1332−1340.